

125 GeV Higgs boson decays in the μ from ν supersymmetric standard model

Hai-Bin Zhang^{a,b,*}, Tai-Fu Feng^{a,b,†}, Fei Sun^{a,b},
Ke-Sheng Sun^{a,b}, Jian-Bin Chen^c, Shu-Min Zhao^{a,‡}

^a*Department of Physics, Hebei University, Baoding, 071002, China*

^b*Department of Physics, Dalian University of Technology, Dalian, 116024, China*

^c*Department of Physics, Taiyuan University of Technology, Taiyuan, 030024, China*

Abstract

Recently the ATLAS and CMS Collaborations have reported significant events that are attributed to the neutral Higgs boson with mass around 125 GeV. In this work, we investigate the signals of the Higgs boson decay channels $h \rightarrow \gamma\gamma$, $h \rightarrow VV^*$ ($V = Z, W$), and $h \rightarrow f\bar{f}$ ($f = b, \tau$) in the μ from ν supersymmetric standard model ($\mu\nu$ SSM). In the numerical results, we show the light stop and stau effects on the signal strengths for the 125 GeV Higgs boson decay channels in the $\mu\nu$ SSM, which can account for the updated experimental data on Higgs.

PACS numbers: 12.60.Jv, 14.80.Da

Keywords: Supersymmetry, Higgs decays

* Corresponding author.

hbzhang@mail.dlut.edu.cn

† fengtf@hbu.edu.cn

‡ smzhao@hbu.edu.cn

I. INTRODUCTION

As the simplest soft broken supersymmetry (SUSY) theory, the minimal supersymmetric standard model (MSSM) [1] has attracted the attention of physicists for a long time. Furthermore, there is the SUSY extension of the standard model (SM), called the “ μ from ν supersymmetric standard model” ($\mu\nu$ SSM) [2–4], which solves the μ problem [5] of the MSSM through the lepton number breaking couplings between the right-handed sneutrinos and the Higgses $\epsilon_{ab}\lambda_i\hat{\nu}_i^c\hat{H}_d^a\hat{H}_u^b$ in the superpotential. Once the electroweak symmetry is broken (EWSB), the effective μ term $\epsilon_{ab}\mu\hat{H}_d^a\hat{H}_u^b$ is generated spontaneously through right-handed sneutrino vacuum expectation values (VEVs), $\mu = \lambda_i\langle\hat{\nu}_i^c\rangle$. Additionally, three tiny neutrino masses are generated at the tree level through a TeV scale seesaw mechanism [2, 6].

To understand the origin of the electroweak symmetry breaking and search for the neutral Higgs [7] predicted by the standard model and its various extensions is the main goal of the Large Hadron Collider (LHC). Recently the ATLAS and CMS Collaborations have reported significant excess events for a new boson, which is interpreted as the neutral Higgs with mass around 125 GeV at 5.0σ level [8, 9]. The CP properties and couplings of the particle are also being established [10, 11]. This implies that the Higgs mechanism to break electroweak symmetry has a solid experimental cornerstone. In this paper, we investigate the 125 GeV Higgs decay channels $h \rightarrow \gamma\gamma$, $h \rightarrow VV^*$ ($V = Z, W$), and $h \rightarrow f\bar{f}$ ($f = b, \tau$) in the $\mu\nu$ SSM. In the numerical analysis, we show the light stop and stau contributions to the signal strengths of the Higgs decay channels.

Our presentation is organized as follows. In Sec. II, we briefly summarize the main ingredients of the $\mu\nu$ SSM by introducing its superpotential and the general soft SUSY-breaking terms, in particular discussing the Higgs sector. We present the decay widths and signal strengths for $h \rightarrow \gamma\gamma$, $h \rightarrow VV^*$ ($V = Z, W$) and $h \rightarrow f\bar{f}$ ($f = b, \tau$) in Sec. III. The numerical analysis are given in Sec. IV, and Sec. V gives a summary. The tedious formulae are collected in Appendixes A–D.

II. THE $\mu\nu$ SSM AND THE HIGGS SECTOR

Besides the superfields of the MSSM, the $\mu\nu$ SSM introduces three singlet right-handed neutrino superfields $\hat{\nu}_i^c$. In addition to the MSSM Yukawa couplings for quarks and charged leptons, the superpotential of the $\mu\nu$ SSM contains Yukawa couplings for neutrinos, two additional types of terms involving the Higgs doublet superfields \hat{H}_d and \hat{H}_u , and the three right-handed neutrino superfields $\hat{\nu}_i^c$, [2]

$$W = \epsilon_{ab} \left(Y_{u_{ij}} \hat{H}_u^b \hat{Q}_i^a \hat{u}_j^c + Y_{d_{ij}} \hat{H}_d^a \hat{Q}_i^b \hat{d}_j^c + Y_{e_{ij}} \hat{H}_d^a \hat{L}_i^b \hat{e}_j^c \right) + \epsilon_{ab} Y_{\nu_{ij}} \hat{H}_u^b \hat{L}_i^a \hat{\nu}_j^c - \epsilon_{ab} \lambda_i \hat{\nu}_i^c \hat{H}_d^a \hat{H}_u^b + \frac{1}{3} \kappa_{ijk} \hat{\nu}_i^c \hat{\nu}_j^c \hat{\nu}_k^c, \quad (1)$$

where $\hat{H}_u^T = (\hat{H}_u^+, \hat{H}_u^0)$, $\hat{H}_d^T = (\hat{H}_d^0, \hat{H}_d^-)$, $\hat{Q}_i^T = (\hat{u}_i, \hat{d}_i)$, $\hat{L}_i^T = (\hat{\nu}_i, \hat{e}_i)$ are $SU(2)$ doublet superfields, and \hat{u}_i^c , \hat{d}_i^c , and \hat{e}_i^c represent the singlet up-type quark, down-type quark and charged lepton superfields, respectively. In addition, $Y_{u,d,e,\nu}$, λ , and κ are dimensionless matrices, a vector, and a totally symmetric tensor. $a, b = 1, 2$ are $SU(2)$ indices with antisymmetric tensor $\epsilon_{12} = 1$, and $i, j, k = 1, 2, 3$ are generation indices. The summation convention is implied on repeated indices in this paper.

In the superpotential, if the scalar potential is such that nonzero VEVs of the scalar components ($\tilde{\nu}_i^c$) of the singlet neutrino superfields $\hat{\nu}_i^c$ are induced, the effective bilinear terms $\epsilon_{ab} \varepsilon_i \hat{H}_u^b \hat{L}_i^a$ and $\epsilon_{ab} \mu \hat{H}_d^a \hat{H}_u^b$ are generated, with $\varepsilon_i = Y_{\nu_{ij}} \langle \tilde{\nu}_j^c \rangle$ and $\mu = \lambda_i \langle \tilde{\nu}_i^c \rangle$, once the electroweak symmetry is broken. The last term generates the effective Majorana masses for neutrinos at the electroweak scale, and the last two terms explicitly violate lepton number and R-parity. In SUSY extensions of the standard model, the R-parity of a particle is defined as $R = (-1)^{L+3B+2S}$ [1] and can be violated if either the baryon number (B) or lepton number (L) is not conserved, where S denotes the spin of concerned component field. R-parity breaking implies that the lightest supersymmetric particle (LSP) is no longer stable. In this context, the neutralino or the sneutrino are no longer candidates for the dark matter. However, other SUSY particles such as the gravitino or the axino can still be used as candidates [3].

In the framework of supergravity-mediated supersymmetry breaking, the general soft

SUSY-breaking terms of the $\mu\nu$ SJM are given by

$$\begin{aligned}
-\mathcal{L}_{soft} = & m_{\tilde{Q}_{ij}}^2 \tilde{Q}_i^{a*} \tilde{Q}_j^a + m_{\tilde{u}_{ij}^c}^2 \tilde{u}_i^{c*} \tilde{u}_j^c + m_{\tilde{d}_{ij}^c}^2 \tilde{d}_i^{c*} \tilde{d}_j^c + m_{\tilde{L}_{ij}}^2 \tilde{L}_i^{a*} \tilde{L}_j^a \\
& + m_{\tilde{e}_{ij}^c}^2 \tilde{e}_i^{c*} \tilde{e}_j^c + m_{H_d}^2 H_d^{a*} H_d^a + m_{H_u}^2 H_u^{a*} H_u^a + m_{\tilde{\nu}_{ij}^c}^2 \tilde{\nu}_i^{c*} \tilde{\nu}_j^c \\
& + \epsilon_{ab} \left[(A_u Y_u)_{ij} H_u^b \tilde{Q}_i^a \tilde{u}_j^c + (A_d Y_d)_{ij} H_d^a \tilde{Q}_i^b \tilde{d}_j^c + (A_e Y_e)_{ij} H_d^a \tilde{L}_i^b \tilde{e}_j^c + \text{H.c.} \right] \\
& + \left[\epsilon_{ab} (A_\nu Y_\nu)_{ij} H_u^b \tilde{L}_i^a \tilde{\nu}_j^c - \epsilon_{ab} (A_\lambda \lambda)_i \tilde{\nu}_i^c H_d^a H_u^b + \frac{1}{3} (A_\kappa \kappa)_{ijk} \tilde{\nu}_i^c \tilde{\nu}_j^c \tilde{\nu}_k^c + \text{H.c.} \right] \\
& - \frac{1}{2} \left(M_3 \tilde{\lambda}_3 \tilde{\lambda}_3 + M_2 \tilde{\lambda}_2 \tilde{\lambda}_2 + M_1 \tilde{\lambda}_1 \tilde{\lambda}_1 + \text{H.c.} \right). \tag{2}
\end{aligned}$$

Here, the first two lines contain mass squared terms of squarks, sleptons, and Higgses. The next two lines consist of the trilinear scalar couplings. In the last line, M_3 , M_2 , and M_1 denote Majorana masses corresponding to $SU(3)$, $SU(2)$, and $U(1)$ gauginos $\hat{\lambda}_3$, $\hat{\lambda}_2$, and $\hat{\lambda}_1$, respectively. In addition to the terms from \mathcal{L}_{soft} , the tree-level scalar potential receives the usual D - and F -term contributions [3].

Once the electroweak symmetry is spontaneously broken, the neutral scalars develop in general the VEVs:

$$\langle H_d^0 \rangle = v_d, \quad \langle H_u^0 \rangle = v_u, \quad \langle \tilde{\nu}_i \rangle = v_{\nu_i}, \quad \langle \tilde{\nu}_i^c \rangle = v_{\nu_i^c}. \tag{3}$$

One can define the neutral scalars as

$$\begin{aligned}
H_d^0 &= \frac{h_d + iP_d}{\sqrt{2}} + v_d, & \tilde{\nu}_i &= \frac{(\tilde{\nu}_i)^\Re + i(\tilde{\nu}_i)^\Im}{\sqrt{2}} + v_{\nu_i}, \\
H_u^0 &= \frac{h_u + iP_u}{\sqrt{2}} + v_u, & \tilde{\nu}_i^c &= \frac{(\tilde{\nu}_i^c)^\Re + i(\tilde{\nu}_i^c)^\Im}{\sqrt{2}} + v_{\nu_i^c},
\end{aligned} \tag{4}$$

and

$$\tan \beta = \frac{v_u}{\sqrt{v_d^2 + v_{\nu_i} v_{\nu_i}}}. \tag{5}$$

For simplicity, we will assume that all parameters in the potential are real. The CP-odd neutral scalar and charged scalar mass matrices can isolate massless unphysical Goldstone bosons G^0 and G^\pm , which can be written as [12, 13]

$$\begin{aligned}
G^0 &= \frac{1}{v_{EW}} \left(v_d P_d - v_u P_u - v_{\nu_i} (\tilde{\nu}_i)^\Im \right), \\
G^\pm &= \frac{1}{v_{EW}} \left(v_d H_d^\pm - v_u H_u^\pm - v_{\nu_i} \tilde{e}_{L_i}^\pm \right),
\end{aligned} \tag{6}$$

through an 8×8 unitary matrix Z_H ,

$$Z_H = \begin{pmatrix} \frac{v_d}{v_{EW}} & \frac{v_u}{v_{SM}} & \left(\frac{v_d v_{\nu_i}}{v_{SM} v_{EW}}\right)_{1 \times 3} \\ -\frac{v_u}{v_{EW}} & \frac{v_d}{v_{SM}} & \left(-\frac{v_u v_{\nu_i}}{v_{SM} v_{EW}}\right)_{1 \times 3} \\ \left(-\frac{v_{\nu_i}}{v_{EW}}\right)_{3 \times 1} & 0_{3 \times 1} & \left(\frac{v_{SM}}{v_{EW}} \delta_{ij} + \varepsilon_{ijk} \frac{v_{\nu_k}}{v_{EW}}\right)_{3 \times 3} \end{pmatrix} \oplus 1_{3 \times 3}, \quad (7)$$

where

$$v_{SM} = \sqrt{v_d^2 + v_u^2}, \quad v_{EW} = \sqrt{v_d^2 + v_u^2 + v_{\nu_i} v_{\nu_i}}. \quad (8)$$

In the physical gauge, the Goldstone bosons G^0 and G^\pm are, respectively, eaten by the Z boson and W boson and disappear from the Lagrangian. The masses squared of the Z boson and W boson are

$$m_Z^2 = \frac{e^2}{2s_W^2 c_W^2} v_{EW}^2, \quad m_W^2 = \frac{e^2}{2s_W^2} v_{EW}^2. \quad (9)$$

Here e is the electromagnetic coupling constant, $s_W = \sin \theta_W$ and $c_W = \cos \theta_W$, with θ_W denoting the Weinberg angle, respectively.

In the $\mu\nu$ SSM, the VEVs of left- and right-handed sneutrinos lead to mixing of the neutral components of the Higgs doublets with the sneutrinos producing an 8×8 CP-even neutral scalar mass matrix. However, if the off-diagonal mixing terms of the CP-even neutral scalar mass matrix are small enough than the diagonal terms, the contribution of the off-diagonal mixing terms to the diagonal doubletlike Higgs masses is small and can be neglected. Actually, we will use this mechanism in our calculation.

Considering radiative corrections, the mass squared matrix for the neutral Higgs doublets in the basis (h_d, h_u) is written as

$$\mathcal{M}^2 = \begin{pmatrix} M_{h_d h_d}^2 + \Delta_{11} & M_{h_d h_u}^2 + \Delta_{12} \\ M_{h_d h_u}^2 + \Delta_{12} & M_{h_u h_u}^2 + \Delta_{22} \end{pmatrix}, \quad (10)$$

with

$$\begin{aligned} M_{h_d h_u}^2 &\simeq -\left[m_A^2 + \left(1 - 4\lambda_i \lambda_i s_W^2 c_W^2 / e^2\right) m_Z^2\right] \sin \beta \cos \beta, \\ M_{h_d h_d}^2 &\simeq m_A^2 \sin^2 \beta + m_Z^2 \cos^2 \beta, \\ M_{h_u h_u}^2 &\simeq m_A^2 \cos^2 \beta + m_Z^2 \sin^2 \beta, \end{aligned} \quad (11)$$

and the neutral pseudoscalar mass squared is

$$m_A^2 \simeq 2[(A_\lambda \lambda)_i v_{\nu_i^c} + \lambda_k \kappa_{ijk} v_{\nu_i^c} v_{\nu_j^c}] / \sin 2\beta. \quad (12)$$

Compared with the MSSM, $M_{h_d h_u}^2$ gets an additional term $(4\lambda_i \lambda_i s_W^2 c_W^2 / e^2) m_Z^2 \sin \beta \cos \beta$, which gives a new contribution to the light doubletlike Higgs mass. In Eq. (10), the concrete expressions for radiative corrections Δ_{11} , Δ_{12} and Δ_{22} can be found in Appendix A. Besides the superfields of the MSSM, the $\mu\nu$ S SM introduces right-handed neutrino superfields. Nevertheless, the loop effects of right-handed neutrino/sneutrino on the light doubletlike Higgs boson mass can be neglected, due to small neutrino Yukawa couplings $Y_{\nu_i} \sim \mathcal{O}(10^{-7})$ and left-handed sneutrino VEVs $v_{\nu_i} \sim \mathcal{O}(10^{-4} \text{ GeV})$. Through the numerical computation, we can ignore the radiative corrections from b quark, τ lepton, and their supersymmetric partners, when $\tan \beta$ is small. The main radiative corrections on the light doubletlike Higgs boson mass come from the top quark and its supersymmetric partners, similarly to the MSSM. By the 2×2 unitary matrix U_h ,

$$U_h = \begin{pmatrix} -\sin \alpha & \cos \alpha \\ \cos \alpha & \sin \alpha \end{pmatrix}, \quad (13)$$

the mass squared matrix \mathcal{M}^2 which contains the radiative corrections can be diagonalized:

$$U_h^T \mathcal{M}^2 U_h = \text{diag}(m_h^2, m_H^2). \quad (14)$$

Here the neutral doubletlike Higgs mass squared eigenvalues $m_{h(H)}^2$ can be derived [14],

$$m_{h(H)}^2 = \frac{1}{2} \left(\text{Tr} \mathcal{M}^2 \mp \sqrt{(\text{Tr} \mathcal{M}^2)^2 - 4 \text{Det} \mathcal{M}^2} \right), \quad (15)$$

where $\text{Tr} \mathcal{M}^2 = \mathcal{M}_{11}^2 + \mathcal{M}_{22}^2$, $\text{Det} \mathcal{M}^2 = \mathcal{M}_{11}^2 \mathcal{M}_{22}^2 - (\mathcal{M}_{12}^2)^2$. The mixing angle α can be determined by [15]

$$\begin{aligned} \sin 2\alpha &= \frac{2\mathcal{M}_{12}^2}{\sqrt{(\text{Tr} \mathcal{M}^2)^2 - 4 \text{Det} \mathcal{M}^2}}, \\ \cos 2\alpha &= \frac{\mathcal{M}_{11}^2 - \mathcal{M}_{22}^2}{\sqrt{(\text{Tr} \mathcal{M}^2)^2 - 4 \text{Det} \mathcal{M}^2}}, \end{aligned} \quad (16)$$

which reduce to $-\sin 2\beta$ and $-\cos 2\beta$, respectively, in the large m_A limit. The convention is that $\pi/4 \leq \beta < \pi/2$ for $\tan \beta \geq 1$, while $-\pi/2 < \alpha < 0$. In the large m_A limit, $\alpha = -\pi/2 + \beta$.

One most stringent constraint on parameter space of the $\mu\nu$ SSM is that the mass squared matrix should produce an eigenvalue around $(125 \text{ GeV})^2$ as mass squared of the light doubletlike Higgs. The combination of the ATLAS [8] and CMS [9] for the neutral Higgs mass gives [16]

$$m_h = 125.7 \pm 0.4 \text{ GeV}. \quad (17)$$

This fact constrains parameter space of the $\mu\nu$ SSM stringently.

III. THE 125 GEV HIGGS DECAYS

At the LHC, the Higgs can be mainly produced by the gluon fusion. In the SM, the leading-order (LO) contributions originate from the one-loop diagrams involving virtual top quark. The cross section for this process is known to the next-to-next-to-leading order (NNLO) [17] which can enhance the LO result by 80%-100%. Beyond the SM, any new particle which strongly couples with the Higgs can modify the cross section of the process significantly. In the new physics (NP), the LO decay width of $h \rightarrow gg$ process is given as (see Ref. [18] and references therein)

$$\Gamma_{\text{NP}}(h \rightarrow gg) = \frac{G_F \alpha_s^2 m_h^3}{64 \sqrt{2} \pi^3} \left| \sum_q g_{hq\bar{q}} A_{1/2}(x_q) + \sum_{\tilde{q}} g_{h\tilde{q}\tilde{q}} \frac{m_Z^2}{m_{\tilde{q}}^2} A_0(x_{\tilde{q}}) \right|^2, \quad (18)$$

with $x_a = m_a^2/(4m_h^2)$, $q = t, b$, and $\tilde{q} = U_I^+, D_I^-$ ($I = 1, \dots, 6$). The concrete expressions of g_{htt} , g_{hbb} , $g_{hU_I^- U_I^+}$, $g_{hD_I^+ D_I^-}$ are formulated as

$$\begin{aligned} g_{htt} &= \frac{\cos \alpha}{\sin \beta}, \\ g_{hbb} &= -\frac{\sin \alpha}{\cos \beta} \sqrt{1 + \sum_{i=1}^3 \frac{v_{\nu_i}^2}{v_d^2}}, \\ g_{hU_I^- U_I^+} &= -\frac{v_{\text{EW}}}{2m_Z^2} C_{1II}^{U^\pm} \quad (I = 1, \dots, 6), \\ g_{hD_I^+ D_I^-} &= -\frac{v_{\text{EW}}}{2m_Z^2} C_{1II}^{D^\pm} \quad (I = 1, \dots, 6), \end{aligned} \quad (19)$$

where the concrete expressions for $C_{1II}^{U^\pm}$, $C_{1II}^{D^\pm}$ can be found in Appendix B. The form factors A_0 , $A_{1/2}$ (and A_1 below) are defined in Appendix C. In Eq. (18), the contributions of

squarks have the damped loop factors $m_Z^2/m_{\tilde{q}}^2$. Thus, contrary to the case of SM quarks, the contributions of squarks become very small for high masses, and the squarks decouple completely from the gluonic Higgs couplings if they are very heavy.

The decay width of the Higgs to diphoton decay at LO in the SM is derived from the one-loop diagrams which contain virtual top quark or virtual W boson. In the NP, the third-generation fermions ($f = t, b, \tau$) and W boson together with the supersymmetric partners give the contributions to the LO decay width for the Higgs to diphoton decay, which can be written by

$$\begin{aligned} \Gamma_{\text{NP}}(h \rightarrow \gamma\gamma) &= \frac{G_F \alpha^2 m_h^3}{128 \sqrt{2} \pi^3} \left| \sum_f N_c Q_f^2 g_{hff} A_{1/2}(x_f) + g_{hWW} A_1(x_W) \right. \\ &\quad + \sum_{\alpha=2}^8 g_{hS_\alpha^+ S_\alpha^-} \frac{m_Z^2}{m_{S_\alpha^\pm}^2} A_0(x_{S_\alpha^\pm}) + \sum_{i=1}^2 g_{h\chi_i^+ \chi_i^-} \frac{m_W}{m_{\chi_i^\pm}} A_{1/2}(x_{\chi_i^\pm}) \\ &\quad \left. + \sum_{\tilde{q}} N_c Q_f^2 g_{h\tilde{q}\tilde{q}} \frac{m_Z^2}{m_{\tilde{q}}^2} A_0(x_{\tilde{q}}) \right|^2, \end{aligned} \quad (20)$$

and the expressions of $g_{h\tau\tau}$, g_{hWW} , $g_{hS_\alpha^+ S_\alpha^-}$, $g_{h\chi_i^+ \chi_i^-}$ are

$$\begin{aligned} g_{h\tau\tau} &\simeq -\frac{\sin \alpha}{\cos \beta} \sqrt{1 + \sum_{i=1}^3 \frac{v_{\nu_i}^2}{v_d^2}}, \\ g_{hWW} &\simeq \sin(\beta - \alpha), \\ g_{hS_\rho^+ S_\rho^-} &= -\frac{v_{EW}}{2m_Z^2} C_{1\rho\rho}^{S^\pm} \quad (\rho = 2, \dots, 8), \\ g_{h\chi_i^+ \chi_i^-} &= -\frac{2}{e} \Re[C_{1ii}^{\chi^\pm}] \quad (i = 1, 2), \end{aligned} \quad (21)$$

where the concrete expressions of $C_{1\rho\rho}^{S^\pm}$, $C_{1ii}^{\chi^\pm}$ can be found in Appendix B. Here, if supersymmetric particles are heavy, the contributions of supersymmetric particles will become small. And then, the main contributions of the Higgs to diphoton decay width at LO is derived from top quark, bottom quark, and W boson.

The light doubletlike Higgs with 125 GeV mass can decay through the channels $h \rightarrow WW^*$, $h \rightarrow ZZ^*$ where V^* ($V = Z, W$) denoting the off-shell electroweak gauge bosons. Summing over all modes available to the W^* or Z^* , the decay widths are given by [19]

$$\begin{aligned} \Gamma_{\text{NP}}(h \rightarrow ZZ^*) &= \frac{e^4 m_h}{2048 \pi^3 s_W^4 c_W^4} |g_{hZZ}|^2 \left(7 - \frac{40}{3} s_W^2 + \frac{160}{9} s_W^4 \right) F\left(\frac{m_Z}{m_h}\right), \\ \Gamma_{\text{NP}}(h \rightarrow WW^*) &= \frac{3e^4 m_h}{512 \pi^3 s_W^4} |g_{hWW}|^2 F\left(\frac{m_W}{m_h}\right), \end{aligned} \quad (22)$$

with $g_{hZZ} = g_{hWW}$ and the form factor $F(x)$ is formulated in Appendix C. The partial decay width of the 125 GeV neutral Higgs into fermion pairs is given in the Born approximation by [20]

$$\Gamma_{\text{NP}}(h \rightarrow f\bar{f}) = N_c \frac{G_F m_f^2 m_h}{4\sqrt{2}\pi} |g_{hff}|^2 (1 - 4m_f^2/m_h^2)^{3/2} \quad (f = b, \tau), \quad (23)$$

with $g_{hbb} \simeq g_{h\tau\tau}$.

Normalized to the SM expectation, the signal strengths for the Higgs decay channels are quantified by the ratios [21]

$$\begin{aligned} \mu_{\gamma\gamma, VV^*}^{\text{ggF}} &= \frac{\sigma_{\text{NP}}(\text{ggF})}{\sigma_{\text{SM}}(\text{ggF})} \frac{\text{BR}_{\text{NP}}(h \rightarrow \gamma\gamma, VV^*)}{\text{BR}_{\text{SM}}(h \rightarrow \gamma\gamma, VV^*)} \quad (V = Z, W), \\ \mu_{f\bar{f}}^{\text{VBF}} &= \frac{\sigma_{\text{NP}}(\text{VBF})}{\sigma_{\text{SM}}(\text{VBF})} \frac{\text{BR}_{\text{NP}}(h \rightarrow f\bar{f})}{\text{BR}_{\text{SM}}(h \rightarrow f\bar{f})} \quad (f = b, \tau), \end{aligned} \quad (24)$$

where ggF and VBF stand for gluon-gluon fusion and vector boson fusion, respectively.

Normalized to the SM values, one can evaluate the Higgs production cross sections

$$\begin{aligned} \frac{\sigma_{\text{NP}}(\text{ggF})}{\sigma_{\text{SM}}(\text{ggF})} &\approx \frac{\Gamma_{\text{NP}}(h \rightarrow gg)}{\Gamma_{\text{SM}}(h \rightarrow gg)} = \frac{\Gamma_{\text{NP}}^h}{\Gamma_{\text{SM}}^h} \frac{\Gamma_{\text{NP}}(h \rightarrow gg)/\Gamma_{\text{NP}}^h}{\Gamma_{\text{SM}}(h \rightarrow gg)/\Gamma_{\text{SM}}^h} \\ &= \frac{\Gamma_{\text{NP}}^h}{\Gamma_{\text{SM}}^h} \frac{\text{BR}_{\text{NP}}(h \rightarrow gg)}{\text{BR}_{\text{SM}}(h \rightarrow gg)}, \\ \frac{\sigma_{\text{NP}}(\text{VBF})}{\sigma_{\text{SM}}(\text{VBF})} &\approx \frac{\Gamma_{\text{NP}}(h \rightarrow VV^*)}{\Gamma_{\text{SM}}(h \rightarrow VV^*)} = \frac{\Gamma_{\text{NP}}^h}{\Gamma_{\text{SM}}^h} \frac{\Gamma_{\text{NP}}(h \rightarrow VV^*)/\Gamma_{\text{NP}}^h}{\Gamma_{\text{SM}}(h \rightarrow VV^*)/\Gamma_{\text{SM}}^h} \\ &= \frac{\Gamma_{\text{NP}}^h}{\Gamma_{\text{SM}}^h} \frac{\text{BR}_{\text{NP}}(h \rightarrow VV^*)}{\text{BR}_{\text{SM}}(h \rightarrow VV^*)}, \end{aligned} \quad (25)$$

with the 125 GeV Higgs total decay width for the NP

$$\begin{aligned} \Gamma_{\text{NP}}^h &= \sum_{f=b,\tau,c,s} \Gamma_{\text{NP}}(h \rightarrow f\bar{f}) + \sum_{V=Z,W} \Gamma_{\text{NP}}(h \rightarrow VV^*) \\ &\quad + \Gamma_{\text{NP}}(h \rightarrow gg) + \Gamma_{\text{NP}}(h \rightarrow \gamma\gamma), \end{aligned} \quad (26)$$

where we have neglected the contributions from the rare or invisible decays, and Γ_{SM}^h denotes the SM Higgs total decay width. Through Eq. (24) and Eq. (25), we can quantify the signal strengths for the Higgs decay channels in the $\mu\nu\text{SSM}$

$$\mu_{\gamma\gamma}^{\text{ggF}} \approx \frac{\Gamma_{\text{NP}}(h \rightarrow gg)}{\Gamma_{\text{SM}}(h \rightarrow gg)} \frac{\Gamma_{\text{NP}}(h \rightarrow \gamma\gamma)/\Gamma_{\text{NP}}^h}{\Gamma_{\text{SM}}(h \rightarrow \gamma\gamma)/\Gamma_{\text{SM}}^h}$$

Signal	Value from ATLAS	Value from CMS	Weighted average
$\mu_{\gamma\gamma}^{\text{ggF}}$	$1.6_{-0.36}^{+0.42}$ [25]	0.52 ± 0.5 [26]	1.19 ± 0.31
$\mu_{ZZ^*}^{\text{ggF}}$	$1.8_{-0.5}^{+0.8}$ [27]	$0.9_{-0.4}^{+0.5}$ [28]	1.18 ± 0.37
$\mu_{WW^*}^{\text{ggF}}$	0.82 ± 0.36 [29]	0.76 ± 0.21 [30]	0.78 ± 0.18

TABLE I: Experimental values for the Higgs decay rates.

$$\begin{aligned}
&= \frac{\Gamma_{\text{SM}}^h}{\Gamma_{\text{NP}}^h} \frac{\Gamma_{\text{NP}}(h \rightarrow gg)}{\Gamma_{\text{SM}}(h \rightarrow gg)} \frac{\Gamma_{\text{NP}}(h \rightarrow \gamma\gamma)}{\Gamma_{\text{SM}}(h \rightarrow \gamma\gamma)}, \\
\mu_{VV^*}^{\text{ggF}} &\approx \frac{\Gamma_{\text{NP}}(h \rightarrow gg)}{\Gamma_{\text{SM}}(h \rightarrow gg)} \frac{\Gamma_{\text{NP}}(h \rightarrow VV^*)/\Gamma_{\text{NP}}^h}{\Gamma_{\text{SM}}(h \rightarrow VV^*)/\Gamma_{\text{SM}}^h} \\
&= \frac{\Gamma_{\text{SM}}^h}{\Gamma_{\text{NP}}^h} \frac{\Gamma_{\text{NP}}(h \rightarrow gg)}{\Gamma_{\text{SM}}(h \rightarrow gg)} |g_{hVV}|^2, \\
\mu_{f\bar{f}}^{\text{VBF}} &\approx \frac{\Gamma_{\text{NP}}(h \rightarrow VV^*)}{\Gamma_{\text{SM}}(h \rightarrow VV^*)} \frac{\Gamma_{\text{NP}}(h \rightarrow f\bar{f})/\Gamma_{\text{NP}}^h}{\Gamma_{\text{SM}}(h \rightarrow f\bar{f})/\Gamma_{\text{SM}}^h} \\
&= \frac{\Gamma_{\text{SM}}^h}{\Gamma_{\text{NP}}^h} |g_{hVV}|^2 |g_{hff}|^2 \quad (V = Z, W; f = b, \tau), \tag{27}
\end{aligned}$$

with $\frac{\Gamma_{\text{NP}}(h \rightarrow VV^*)}{\Gamma_{\text{SM}}(h \rightarrow VV^*)} = |g_{hVV}|^2 = |g_{hZZ}|^2 = |g_{hWW}|^2$ and $\frac{\Gamma_{\text{NP}}(h \rightarrow f\bar{f})}{\Gamma_{\text{SM}}(h \rightarrow f\bar{f})} = |g_{hff}|^2 = |g_{hbb}|^2 \simeq |g_{h\tau\tau}|^2$. Therefore, we could just analyze the signal strengths $\mu_{\gamma\gamma}^{\text{ggF}}$, $\mu_{VV^*}^{\text{ggF}}$ and $\mu_{f\bar{f}}^{\text{VBF}}$ in the following.

The latest LHC measurements of the Higgs decay rates are summarized in Table I, where we also compute the weighted averages for the signal strengths $\mu_{\gamma\gamma, VV^*}^{\text{ggF}}$ ($V = Z, W$) from ATLAS and CMS. When the errors are asymmetric, we average them in quadrature. Note that for the signal strengths $\mu_{\gamma\gamma, ZZ^*}^{\text{ggF}}$, the average from ATLAS and CMS just is used as a guideline, but this should be taken with some care as the two experiments have quite different central values. As the signal strengths $\mu_{ZZ^*}^{\text{ggF}}$ and $\mu_{WW^*}^{\text{ggF}}$ depend on the same couplings, we combine them and give a weighted average

$$\mu_{VV^*}^{\text{ggF}} = 0.86 \pm 0.16, \tag{28}$$

to constrain the numerical evolution of $\mu_{VV^*}^{\text{ggF}}$ in the following. Since the measured rates for the channels $h \rightarrow f\bar{f}$ still have large experimental error at now [22–24], here we will not consider their experimental values to constrain the channels $h \rightarrow f\bar{f}$ in the $\mu\nu\text{SSM}$.

IV. NUMERICAL ANALYSIS

There are many free parameters in the SUSY extensions of the SM. In order to obtain a transparent numerical results, we make some assumptions on parameter space for the $\mu\nu$ SJM before performing the numerical calculation. In the following, we make the minimal flavor violation (MFV) assumption

$$\begin{aligned}
\kappa_{ijk} &= \kappa\delta_{ij}\delta_{jk}, & (A_\kappa\kappa)_{ijk} &= A_\kappa\kappa\delta_{ij}\delta_{jk}, & \lambda_i &= \lambda, & (A_\lambda\lambda)_i &= A_\lambda\lambda, \\
Y_{u_{ij}} &= Y_{u_i}\delta_{ij}, & (A_u Y_u)_{ij} &= A_{u_i}Y_{u_i}\delta_{ij}, & Y_{\nu_{ij}} &= Y_{\nu_i}\delta_{ij}, & (A_\nu Y_\nu)_{ij} &= a_{\nu_i}\delta_{ij}, \\
Y_{d_{ij}} &= Y_{d_i}\delta_{ij}, & (A_d Y_d)_{ij} &= A_{d_i}Y_{d_i}\delta_{ij}, & Y_{e_{ij}} &= Y_{e_i}\delta_{ij}, & (A_e Y_e)_{ij} &= A_{e_i}Y_{e_i}\delta_{ij}, \\
m_{\tilde{L}_{ij}}^2 &= m_{\tilde{L}_i}^2\delta_{ij}, & m_{\tilde{\nu}_i^c}^2 &= m_{\tilde{\nu}_i}^2\delta_{ij}, & m_{\tilde{e}_i^c}^2 &= m_{\tilde{e}_i}^2\delta_{ij}, & \nu_{\nu_i^c} &= \nu_{\nu^c}, \\
m_{\tilde{Q}_{ij}}^2 &= m_{\tilde{Q}_i}^2\delta_{ij}, & m_{\tilde{u}_i^c}^2 &= m_{\tilde{u}_i}^2\delta_{ij}, & m_{\tilde{d}_i^c}^2 &= m_{\tilde{d}_i}^2\delta_{ij}, & &
\end{aligned} \tag{29}$$

where $i, j, k = 1, 2, 3$.

Restrained by the quark and lepton masses, we have

$$Y_{u_i} = \frac{m_{u_i}}{v_u}, \quad Y_{d_i} = \frac{m_{d_i}}{v_d}, \quad Y_{e_i} = \frac{m_{l_i}}{v_d}, \tag{30}$$

where m_{u_i} , m_{d_i} and m_{l_i} are the up-quark, down-quark and charged lepton masses, respectively, and the values are taken from the PDG [31]. For the masses of bino and wino, we will imply the approximate GUT relation $M_1 = \frac{\alpha_1^2}{\alpha_2}M_2 \approx 0.5M_2$. In Appendix D, the tree-level tadpoles, Eqs. (D2)–(D5), are set to be zero to minimize the potential. In this way, the soft masses $m_{\tilde{H}_d}^2$, $m_{\tilde{H}_u}^2$ and $m_{\tilde{\nu}_i^c}^2$ can be derived. Simultaneously, ignoring the terms of the second order in Y_ν and assuming $(v_{\nu_i}^2 + v_d^2 - v_u^2) \approx (v_d^2 - v_u^2)$, one can solve the minimization conditions of the neutral scalar potential with respect to v_{ν_i} ($i = 1, 2, 3$) as [6]:

$$v_{\nu_i} = \frac{\lambda v_d(v_u^2 + v_{\nu^c}^2) - \kappa v_u v_{\nu^c}^2}{m_{\tilde{L}_i}^2 + \frac{G^2}{4}(v_d^2 - v_u^2)} Y_{\nu_i} - \frac{v_u v_{\nu^c}}{m_{\tilde{L}_i}^2 + \frac{G^2}{4}(v_d^2 - v_u^2)} a_{\nu_i}, \tag{31}$$

where $G^2 = g_1^2 + g_2^2$ and $g_1 c_W = g_2 s_W = e$.

In the $\mu\nu$ SJM, the masses of left-handed sneutrinos are basically determined by $m_{\tilde{L}_i}$, and the three right-handed sneutrinos are essentially degenerated. The CP-even and CP-odd right-handed sneutrinos mass squared $m_{S_{5+i}}^2$ and $m_{P_{5+i}}^2$ could be approximately written as

$$m_{S_{5+i}}^2 \approx (A_\kappa + 4\kappa\nu_{\nu^c})\kappa\nu_{\nu^c} + A_\lambda\lambda v_d v_u / \nu_{\nu^c} - 2\lambda^2(v_d^2 + v_u^2),$$

$$m_{P_{5+i}}^2 \approx -3A_\kappa \kappa v_{\nu^c} + (A_\lambda/v_{\nu^c} + 4\kappa)\lambda v_d v_u - 2\lambda^2(v_d^2 + v_u^2). \quad (32)$$

Here, the main contribution to the mass squared is the first term as κ is large, due to $v_{\nu^c} \gg v_{u,d}$. Therefore, we could use the approximate relation

$$-4\kappa v_{\nu^c} \lesssim A_\kappa \lesssim 0 \quad (33)$$

to avoid the tachyons.

Before the numerical calculation, the constraints on the parameters of the $\mu\nu$ SSM from neutrino experiments should be considered at first. Three flavor neutrinos $\nu_{e,\mu,\tau}$ could mix into three massive neutrinos $\nu_{1,2,3}$ during their flight, and the mixing is described by the Pontecorvo-Maki-Nakagawa-Sakata unitary matrix U_{PMNS} [32]. Through several recent reactor oscillation experiments [33], θ_{13} is now precisely known. The global fit of θ_{13} gives [34]

$$\sin^2 \theta_{13} = 0.023 \pm 0.0023. \quad (34)$$

The other experimental observations of the parameters in U_{PMNS} for the normal mass hierarchy [34] show that

$$\begin{aligned} \sin^2 \theta_{12} &= 0.302_{-0.012}^{+0.013}, & \Delta m_{21}^2 &= 7.50_{-0.19}^{+0.18} \times 10^{-5} \text{eV}^2, \\ \sin^2 \theta_{23} &= 0.413_{-0.025}^{+0.037}, & \Delta m_{31}^2 &= 2.473_{-0.067}^{+0.070} \times 10^{-3} \text{eV}^2. \end{aligned} \quad (35)$$

In the $\mu\nu$ SSM, the three neutrino masses are obtained through a TeV scale seesaw mechanism [2, 6]. Assuming that the charged lepton mass matrix in the flavor basis is in the diagonal form, we parametrize the unitary matrix which diagonalizes the effective neutrino mass matrix m_{eff} (see Ref. [12]) as [35]

$$\begin{aligned} U_\nu &= \begin{pmatrix} c_{12}c_{13} & s_{12}c_{13} & s_{13}e^{-i\delta} \\ -s_{12}c_{23} - c_{12}s_{23}s_{13}e^{i\delta} & c_{12}c_{23} - s_{12}s_{23}s_{13}e^{i\delta} & s_{23}c_{13} \\ s_{12}s_{23} - c_{12}c_{23}s_{13}e^{i\delta} & -c_{12}s_{23} - s_{12}c_{23}s_{13}e^{i\delta} & c_{23}c_{13} \end{pmatrix} \\ &\times \text{diag}(1, e^{i\frac{\alpha_{21}}{2}}, e^{i\frac{\alpha_{31}}{2}}), \end{aligned} \quad (36)$$

where $c_{ij} = \cos \theta_{ij}$, $s_{ij} = \sin \theta_{ij}$. In the next calculation, the values of θ_{ij} are obtained from the experimental data in Eq. (34) and Eq. (35), and all CP violating phases δ , α_{21} , and α_{31}

are set to zero. The unitary matrix U_ν diagonalizes the effective neutrino mass matrix m_{eff} in the following way:

$$U_\nu^T m_{eff}^T m_{eff} U_\nu = \text{diag}(m_{\nu_1}^2, m_{\nu_2}^2, m_{\nu_3}^2). \quad (37)$$

For the neutrino mass spectrum, we assume it to be normal hierarchical, i.e., $m_{\nu_1} < m_{\nu_2} < m_{\nu_3}$, and we choose the lightest neutrino mass $m_{\nu_1} = 10^{-2}$ eV as input in our numerical analysis, limited by neutrino masses from neutrinoless double- β decay [36] and cosmology [37]. The other two neutrino masses $m_{\nu_{2,3}}$ can be obtained through the experimental data on the differences of neutrino mass squared in Eq. (35). Then we can numerically derive $Y_{\nu_i} \sim \mathcal{O}(10^{-7})$ and $a_{\nu_i} \sim \mathcal{O}(-10^{-4}\text{GeV})$ from Eq. (37). Accordingly, $v_{\nu_i} \sim \mathcal{O}(10^{-4}\text{GeV})$ through Eq. (31). Due to $v_{\nu_i} \ll v_{u,d}$, we can have

$$\tan \beta \simeq \frac{v_u}{v_d}. \quad (38)$$

We also impose a constraint on the SUSY contribution to the muon anomalous magnetic dipole moment a_μ in the $\mu\nu\text{SSM}$ [12]. The difference between experiment and the SM prediction on a_μ is [31, 38]

$$\Delta a_\mu = a_\mu^{\text{exp}} - a_\mu^{\text{SM}} = (24.8 \pm 7.9) \times 10^{-10}, \quad (39)$$

with all errors combined in quadrature. Therefore, the SUSY contribution to a_μ in the $\mu\nu\text{SSM}$ should be constrained as $1.1 \times 10^{-10} \leq \Delta a_\mu \leq 48.5 \times 10^{-10}$, where a 3σ experimental error is considered. In Ref. [12], we can know that the experimental data for a_μ will give a large constraint on the parameter M_2 , for a given value of $\tan \beta$.

For relevant parameters in the SM, we choose [31]

$$\begin{aligned} \alpha_s(m_Z) &= 0.118, & m_t &= 173.5 \text{ GeV}, & m_Z &= 91.188 \text{ GeV}, \\ \alpha(m_Z) &= 1/128, & m_b &= 4.65 \text{ GeV}, & m_W &= 80.385 \text{ GeV}. \end{aligned} \quad (40)$$

Through the analysis of the parameter space in Ref. [3], we could choose the reasonable values for some parameters in the $\mu\nu\text{SSM}$ as $\kappa = 0.4$, $A_\kappa = -300$ GeV, and $A_\lambda = 500$ GeV for simplicity. Here we choose small A_κ to avoid the tachyons, through Eq. (33). We assume that the first two generations of squarks and the right-handed sbottom are heavy,

Parameters	Min	Max	Step
$\tan \beta$	2	30	7
λ	0.1	0.2	0.05
v_{ν^c}/TeV	1	3	1
M_2/TeV	0.5	3.5	1
A_t/TeV	-2.6	3.4	0.1
$m_{\tilde{u}_3^c}/\text{GeV}$	100	800	20

TABLE II: Scanning parameters for the light stop effect on the Higgs decays.

$m_{\tilde{Q}_{1,2}} = m_{\tilde{u}_{1,2}^c} = m_{\tilde{d}_{1,2,3}^c} = 2$ TeV, because they play a minor role for the Higgs physics. For simplicity, we can choose $m_{\tilde{L}_{1,2}} = m_{\tilde{e}_{1,2}^c} = 1$ TeV and $A_{e_{1,2,3}} = A_{d_{1,2,3}} = A_{u_{1,2}} = 1$ TeV. As key parameters, $m_{\tilde{Q}_3}$, $m_{\tilde{u}_3^c}$ and $A_{u_3} \equiv A_t$, affects the 125 GeV Higgs mass and decays.

Stops have been searched for at the LHC in gauge-mediated SUSY breaking (GMSB) models [39], where the gravitino (\tilde{G}) is typically the LSP which is similar to the $\mu\nu\text{SSM}$. These studies rule out stop masses up to 200–600 GeV, where the light stop \tilde{t}_1 might decay via $b\tilde{\chi}_1^\pm$, $t\tilde{\chi}_1^0$ and $\tilde{\chi}_1^0$ decay in $Z(h)\tilde{G}$. These studies assumed that the lightest neutralino mass is less than the light stop mass, $m_{\tilde{\chi}_1^0} < m_{\tilde{t}_1}$. The $m_{\tilde{\chi}_1^0} > m_{\tilde{t}_1}$ case still needs be tested in the future. So, for $m_{\tilde{\chi}_1^0} > m_{\tilde{t}_1}$, we still could consider $m_{\tilde{t}_1} < 600$ GeV to study the light stop effect on Higgs decays in the $\mu\nu\text{SSM}$. Constrained by the 125 GeV Higgs, we could have a several TeV heavy stop and a several hundred GeV light stop. To keep the left-handed sbottom heavy, we choose $m_{\tilde{Q}_3} \gg m_{\tilde{u}_3^c}$ [40]. In the following, we take $m_{\tilde{Q}_3} = 2$ TeV for simplicity. So, here the heavy stop mass $m_{\tilde{t}_2}$ is around 2 TeV. Then, the free parameters that affect our next analysis are

$$\tan \beta, \lambda, v_{\nu^c}, M_2, A_t, m_{\tilde{u}_3^c}, m_{\tilde{L}_3}, m_{\tilde{e}_3^c}. \quad (41)$$

Taking $m_{\tilde{L}_3} = m_{\tilde{e}_3^c} = 1$ TeV to ignore the light stau effect, we study the light stop effect on Higgs decays in the $\mu\nu\text{SSM}$ in Fig. 1, by scanning the parameters listed in Table II. In Table II, we take relatively small value of the parameter λ , considering the Landau pole condition at the high-energy scale [3]. In the scanning, we avoid the tachyons, simultaneously coinciding with $m_{\tilde{\chi}_1^0} > m_{\tilde{t}_1}$, and the heavy doubletlike Higgs mass $m_H \geq 642$ GeV [41].

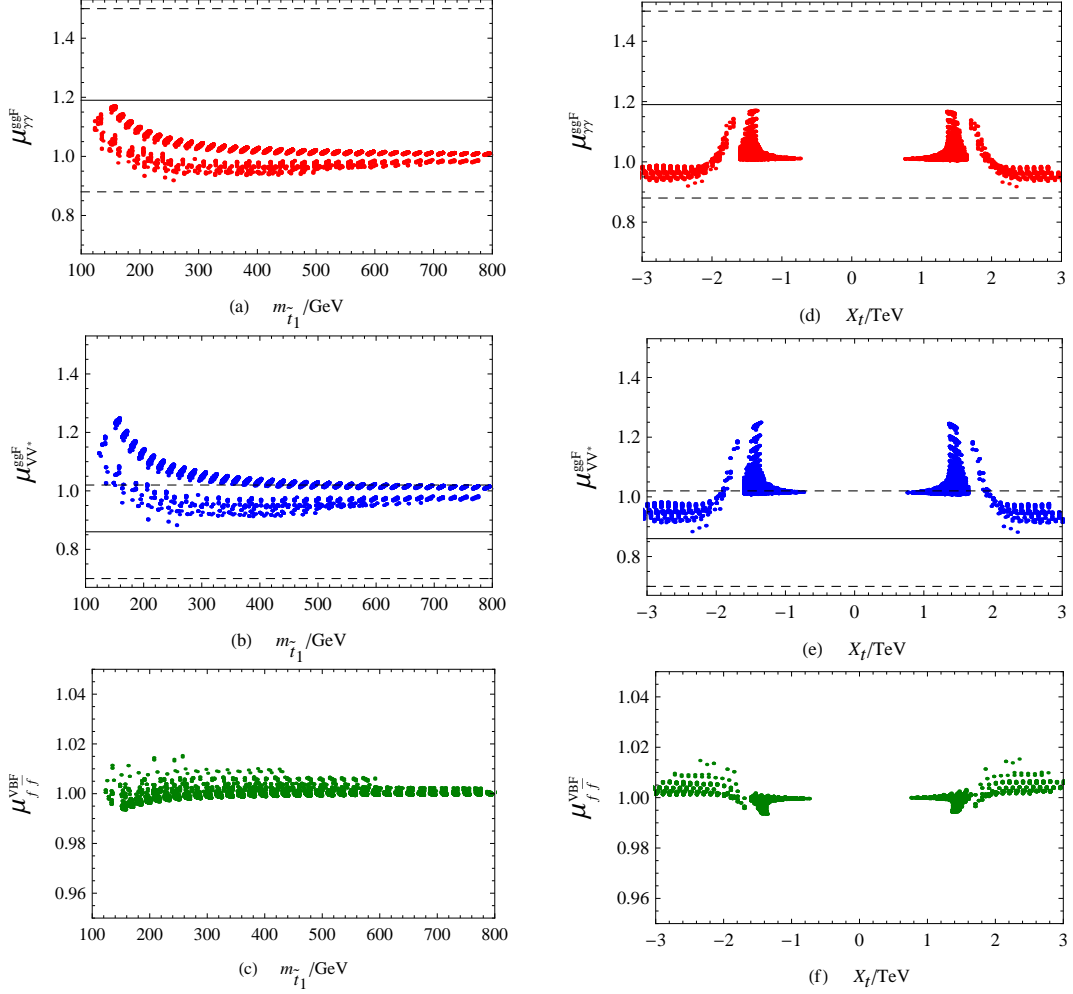


FIG. 1: (Color online) $\mu_{\gamma\gamma}^{\text{ggF}}$ (a),(d), $\mu_{VV^*}^{\text{ggF}}$ (b),(e) and $\mu_{f\bar{f}}^{\text{VBF}}$ (c),(f) vary with $m_{\tilde{t}_1}$ and $X_t = A_t - \mu/\tan\beta$, respectively, where the horizontal solid lines correspond to the experimental central values and the dashed lines to the 1σ intervals.

The results are also constrained by the light doubletlike Higgs mass with $124.5 \text{ GeV} \leq m_h \leq 126.9 \text{ GeV}$ and the muon anomalous magnetic dipole moment $1.1 \times 10^{-10} \leq \Delta a_\mu \leq 48.5 \times 10^{-10}$, where a 3σ experimental error is considered.

In Fig. 1, we plot the signal strengths $\mu_{\gamma\gamma}^{\text{ggF}}$ (a), $\mu_{VV^*}^{\text{ggF}}$ (b), and $\mu_{f\bar{f}}^{\text{VBF}}$ (c) varying with the light stop mass $m_{\tilde{t}_1}$, respectively, where the horizontal solid lines correspond to the experimental central values and the dashed lines to the 1σ intervals. The numerical results show that the light stop could give large effect on the signal strengths $\mu_{\gamma\gamma}^{\text{ggF}}$ and $\mu_{VV^*}^{\text{ggF}}$, as the light stop mass is small. With increasing of the light stop mass, the contribution of the light

Parameters	Min	Max	Step
$\tan \beta$	30	60	5
λ	0.1	0.2	0.05
$\nu_{\nu c}/\text{TeV}$	1	3	0.2
M_2/TeV	0.5	3.5	1.5
A_t/TeV	-2.6	3.4	0.2
$m_{\tilde{e}_3^c}/\text{GeV}$	100	400	30

TABLE III: Scanning parameters for the light stau effect on the Higgs to diphoton decay.

stop for the signal strengths become small. When $m_{\tilde{t}_1} \gtrsim 700$ GeV, the signal strengths $\mu_{\gamma\gamma}^{\text{ggF}}$ and $\mu_{VV^*}^{\text{ggF}}$ are close to 1, which is in agreement with the SM. Fig. 1(c) indicates the light stop play a minor role for the signal strength $\mu_{f\bar{f}}^{\text{VBF}}$.

To explain the results of the signal strengths further, in Fig. 1 we also plot the signal strengths $\mu_{\gamma\gamma}^{\text{ggF}}$ (d), $\mu_{VV^*}^{\text{ggF}}$ (e), and $\mu_{f\bar{f}}^{\text{VBF}}$ (f), respectively, versus $X_t = A_t - \mu/\tan\beta$, where $\mu = 3\lambda\nu_{\nu c}$. One can find that the signal strengths $\mu_{\gamma\gamma, VV^*}^{\text{ggF}} > 1$ when $|X_t| \lesssim 2$ TeV and $\mu_{\gamma\gamma, VV^*}^{\text{ggF}} < 1$ for $|X_t| \gtrsim 2$ TeV. This shows that the light stop effect can be of either sign, depending on the parameter $X_t = A_t - \mu/\tan\beta$, as we will discuss in detail below. Coinciding with the MSSM, the stop loop contributions to the gg or $\gamma\gamma$ amplitude in the $\mu\nu\text{SSM}$ can be approximately proportional to [42–46]

$$\Delta\mathcal{A}_{gg, \gamma\gamma}^{\tilde{t}} \propto \frac{m_{\tilde{t}}^2}{m_{\tilde{t}_1}^2 m_{\tilde{t}_2}^2} (m_{\tilde{t}_1}^2 + m_{\tilde{t}_2}^2 - X_t^2), \quad (42)$$

For $X_t^2 < (m_{\tilde{t}_1}^2 + m_{\tilde{t}_2}^2)$, the stops lead to an enhancement of the gluon-gluon Higgs production. So, the signal strengths $\mu_{\gamma\gamma, VV^*}^{\text{ggF}} > 1$, when $|X_t| < \sqrt{(m_{\tilde{t}_1}^2 + m_{\tilde{t}_2}^2)} \sim 2$ TeV. In Fig. 1, the signal strength $\mu_{VV^*}^{\text{ggF}}$ can reach 1.25; however, the signal strength $\mu_{\gamma\gamma}^{\text{ggF}}$ just reaches 1.17, since the stops lead to a reduction of the Higgs to diphoton decay width for $X_t^2 < (m_{\tilde{t}_1}^2 + m_{\tilde{t}_2}^2)$. On the contrary, the stops reduce the signal strengths $\mu_{\gamma\gamma}^{\text{ggF}}$ and $\mu_{VV^*}^{\text{ggF}}$, when $X_t^2 > (m_{\tilde{t}_1}^2 + m_{\tilde{t}_2}^2)$. Additionally, the signal strength $\mu_{f\bar{f}}^{\text{VBF}} < 1$ as $|X_t| \lesssim 2$ TeV and $\mu_{f\bar{f}}^{\text{VBF}} > 1$ when $|X_t| \gtrsim 2$ TeV, is due to be rescaled by the total width $\Gamma_{\text{SM}}^h/\Gamma_{\text{NP}}^h$ in Eq. (27).

Taking $m_{\tilde{u}_3^c} = 1$ TeV to ignore the stop effect and choosing $m_{\tilde{L}_3} = 0.5$ TeV to keep the third generation of left-handed sneutrinos relatively heavy, we study the light stau effect on

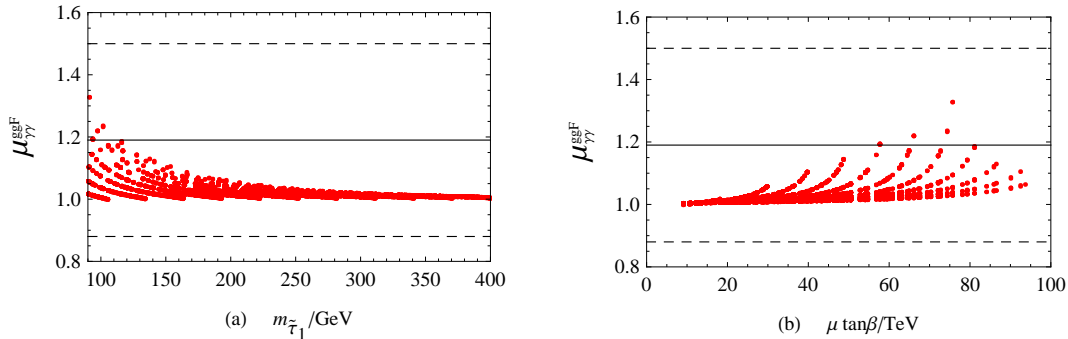


FIG. 2: (Color online) $\mu_{\gamma\gamma}^{\text{ggF}}$ vary with $m_{\tilde{\tau}_1}$ (a) and $\mu \tan \beta$ (b), respectively, where the horizontal solid lines correspond to the experimental central values given in Table I and the dashed lines to the 1σ intervals.

the Higgs to diphoton decay in the $\mu\nu\text{SSM}$ in Fig. 2, where we scan the parameter space listed in Table III. In the scanning, the results are also constrained by the heavy doubletlike Higgs mass $m_H \geq 642$ GeV, the light doubletlike Higgs mass with $124.5 \text{ GeV} \leq m_h \leq 126.9$ GeV, and the muon anomalous magnetic dipole moment. Here we consider the constraint of the light stau mass $m_{\tilde{\tau}_1} \gtrsim 90$ GeV from the LEP limit. In Fig. 2, we plot the signal strength $\mu_{\gamma\gamma}^{\text{ggF}}$ varying with the light stau mass $m_{\tilde{\tau}_1}$ (a) and $\mu \tan \beta$ (b), respectively. Figure 2(a) shows that the light stau can give a large enhancement on the signal strength $\mu_{\gamma\gamma}^{\text{ggF}}$, when $m_{\tilde{\tau}_1} \lesssim 300$ GeV. Figure 2(b) indicates that the signal strength $\mu_{\gamma\gamma}^{\text{ggF}}$ is enhanced greatly, as $\mu \tan \beta$ is large because large values of μ and $\tan \beta$ induce large mixing in the stau sector leading to an enhancement of the Higgs to diphoton decay width [43, 46, 47].

V. SUMMARY

In the framework of the $\mu\nu\text{SSM}$, we attempt to account for the experimental data on the Higgs reported by ATLAS and CMS recently. Under some assumptions and constraints of the parameter space, the results indicate that the 125 GeV Higgs decay signal strengths $\mu_{\gamma\gamma}^{\text{ggF}}$, $\mu_{VV^*}^{\text{ggF}}$ ($V = Z, W$) and μ_{ff}^{VBF} ($f = b, \tau$) can fit the experimental data. Meanwhile, the numerical evaluations on the heavy doubletlike Higgs mass m_H exceed 642 GeV.

In the $\mu\nu\text{SSM}$, we show the light stop and stau contributions to the 125 GeV Higgs decay signal strengths. The light stop leads to an enhancement or reduction of the signal

strengths $\mu_{\gamma\gamma}^{\text{ggF}}$ and $\mu_{VV^*}^{\text{ggF}}$. The signal strength $\mu_{f\bar{f}}^{\text{VBF}}$ is consistent with the SM. For large μ and $\tan\beta$, the light stau could considerably enhance the signal strength $\mu_{\gamma\gamma}^{\text{ggF}}$. Note that for the signal strengths $\mu_{\gamma\gamma,ZZ^*}^{\text{ggF}}$, ATLAS and CMS report currently quite different central values, as indicated in Table I. Here the average of the two values is just used as a rough guideline. In the near future, further constraints can be obtained from more precise determinations of the signal strengths in the measured decay channels at the LHC.

Acknowledgements

This work has been supported by the National Natural Science Foundation of China (NNSFC) with Grants No. 11275036 and No. 11047002, the open project of State Key Laboratory of Mathematics-Mechanization with Grant No. Y3KF311CJ1, the Natural Science Foundation of Hebei province with Grant No. A2013201277, and the Natural Science Fund of Hebei University with Grants No. 2011JQ05 and No. 2012-242.

Appendix A: The radiative corrections

The radiative corrections on the doubletlike Higgses originate from fermions and corresponding supersymmetric partners in the $\mu\nu\text{SSM}$:

$$\begin{aligned}\Delta_{11} &= \Delta_{11}^t + \Delta_{11}^b + \Delta_{11}^l, \\ \Delta_{12} &= \Delta_{12}^t + \Delta_{11}^b + \Delta_{12}^l, \\ \Delta_{22} &= \Delta_{22}^t + \Delta_{11}^b + \Delta_{22}^l.\end{aligned}\tag{A1}$$

Neglecting the terms containing small coupling Y_{ν_i} and v_{ν_i} , and using the expressions given in Ref. [48], the radiative corrections from the top quark and its scalar partner $\tilde{t}_{1,2}$ including two-loop leading-log effects [14] read as

$$\begin{aligned}\Delta_{11}^t &= \frac{3G_F m_t^4}{2\sqrt{2}\pi^2 \sin^2\beta} \frac{\mu^2 (A_t - \mu \cot\beta)^2}{(m_{\tilde{t}_1}^2 - m_{\tilde{t}_2}^2)^2} g(m_{\tilde{t}_1}^2, m_{\tilde{t}_2}^2), \\ \Delta_{12}^t &= \frac{3G_F m_t^4}{2\sqrt{2}\pi^2 \sin^2\beta} \frac{\mu(-A_t + \mu \cot\beta)}{m_{\tilde{t}_1}^2 - m_{\tilde{t}_2}^2} \left\{ \ln \frac{m_{\tilde{t}_1}^2}{m_{\tilde{t}_2}^2} + \frac{A_t(A_t - \mu \cot\beta)}{(m_{\tilde{t}_1}^2 - m_{\tilde{t}_2}^2)} g(m_{\tilde{t}_1}^2, m_{\tilde{t}_2}^2) \right\},\end{aligned}$$

$$\begin{aligned}
\Delta_{22}^t = & \frac{3G_F m_t^4}{2\sqrt{2}\pi^2 \sin^2 \beta} \left\{ \ln \frac{m_{\tilde{t}_1}^2 m_{\tilde{t}_2}^2}{m_t^4} + \frac{2A_t(A_t - \mu \cot \beta)}{m_{\tilde{t}_1}^2 - m_{\tilde{t}_2}^2} \ln \frac{m_{\tilde{t}_1}^2}{m_{\tilde{t}_2}^2} \right. \\
& + \frac{A_t^2(A_t - \mu \cot \beta)^2}{(m_{\tilde{t}_1}^2 - m_{\tilde{t}_2}^2)^2} g(m_{\tilde{t}_1}^2, m_{\tilde{t}_2}^2) + \frac{1}{16\pi^2} \ln \frac{m_{\tilde{t}_1}^2 m_{\tilde{t}_2}^2}{m_t^4} \left(\frac{3e^2 m_t^2}{4s_W^2 m_W^2} - 32\pi\alpha_s \right) \\
& \left. \times \left[\frac{1}{2} \ln \frac{m_{\tilde{t}_1}^2 m_{\tilde{t}_2}^2}{m_t^4} + \frac{2(A_t - \mu \cot \beta)^2}{m_{\tilde{t}_1} m_{\tilde{t}_2}} \left(1 - \frac{(A_t - \mu \cot \beta)^2}{12m_{\tilde{t}_1} m_{\tilde{t}_2}} \right) \right] \right\}, \tag{A2}
\end{aligned}$$

with

$$g(m_1^2, m_2^2) = 2 - \frac{m_1^2 + m_2^2}{m_1^2 - m_2^2} \ln \frac{m_1^2}{m_2^2}. \tag{A3}$$

The one-loop radiative corrections from the bottom quark and its scalar partner $\tilde{b}_{1,2}$ are formulated as

$$\begin{aligned}
\Delta_{11}^b = & \frac{3G_F m_b^4}{2\sqrt{2}\pi^2 \cos^2 \beta} \left\{ \ln \frac{m_{\tilde{b}_1}^2 m_{\tilde{b}_2}^2}{m_b^4} + \frac{2A_b(A_b - \mu \tan \beta)}{m_{\tilde{b}_1}^2 - m_{\tilde{b}_2}^2} \ln \frac{m_{\tilde{b}_1}^2}{m_{\tilde{b}_2}^2} \right. \\
& \left. + \frac{A_b^2(A_b - \mu \tan \beta)^2}{(m_{\tilde{b}_1}^2 - m_{\tilde{b}_2}^2)^2} g(m_{\tilde{b}_1}^2, m_{\tilde{b}_2}^2) \right\}, \\
\Delta_{12}^b = & \frac{3G_F m_b^4}{2\sqrt{2}\pi^2 \cos^2 \beta} \frac{\mu(-A_b + \mu \tan \beta)}{m_{\tilde{b}_1}^2 - m_{\tilde{b}_2}^2} \left\{ \ln \frac{m_{\tilde{b}_1}^2}{m_{\tilde{b}_2}^2} + \frac{A_b(A_b - \mu \tan \beta)}{(m_{\tilde{b}_1}^2 - m_{\tilde{b}_2}^2)} g(m_{\tilde{b}_1}^2, m_{\tilde{b}_2}^2) \right\}, \\
\Delta_{22}^b = & \frac{3G_F m_b^4}{2\sqrt{2}\pi^2 \cos^2 \beta} \frac{\mu^2(A_b - \mu \tan \beta)^2}{(m_{\tilde{b}_1}^2 - m_{\tilde{b}_2}^2)^2} g(m_{\tilde{b}_1}^2, m_{\tilde{b}_2}^2), \tag{A4}
\end{aligned}$$

Similarly, one can obtain the one-loop radiative corrections from the τ lepton and its scalar partner $\tilde{\tau}_{1,2}$:

$$\begin{aligned}
\Delta_{11}^l = & \frac{G_F m_\tau^4}{2\sqrt{2}\pi^2 \cos^2 \beta} \left\{ \ln \frac{m_{\tilde{\tau}_1}^2 m_{\tilde{\tau}_2}^2}{m_\tau^4} + \frac{2A_\tau(A_\tau - \mu \tan \beta)}{m_{\tilde{\tau}_1}^2 - m_{\tilde{\tau}_2}^2} \ln \frac{m_{\tilde{\tau}_1}^2}{m_{\tilde{\tau}_2}^2} \right. \\
& \left. + \frac{A_\tau^2(A_\tau - \mu \tan \beta)^2}{(m_{\tilde{\tau}_1}^2 - m_{\tilde{\tau}_2}^2)^2} g(m_{\tilde{\tau}_1}^2, m_{\tilde{\tau}_2}^2) \right\}, \\
\Delta_{12}^l = & \frac{G_F m_\tau^4}{2\sqrt{2}\pi^2 \cos^2 \beta} \frac{\mu(-A_\tau + \mu \tan \beta)}{m_{\tilde{\tau}_1}^2 - m_{\tilde{\tau}_2}^2} \left\{ \ln \frac{m_{\tilde{\tau}_1}^2}{m_{\tilde{\tau}_2}^2} + \frac{A_\tau(A_\tau - \mu \tan \beta)}{(m_{\tilde{\tau}_1}^2 - m_{\tilde{\tau}_2}^2)} g(m_{\tilde{\tau}_1}^2, m_{\tilde{\tau}_2}^2) \right\}, \\
\Delta_{22}^l = & \frac{G_F m_\tau^4}{2\sqrt{2}\pi^2 \cos^2 \beta} \frac{\mu^2(A_\tau - \mu \tan \beta)^2}{(m_{\tilde{\tau}_1}^2 - m_{\tilde{\tau}_2}^2)^2} g(m_{\tilde{\tau}_1}^2, m_{\tilde{\tau}_2}^2). \tag{A5}
\end{aligned}$$

Appendix B: The couplings

The couplings of CP-even neutral scalars and charged scalars are formulated as

$$\mathcal{L}_{int} = \sum_{\alpha,\beta,\gamma=1}^8 C_{\alpha\beta\gamma}^{S^\pm} S_\alpha S_\beta^+ S_\gamma^-, \quad (\text{B1})$$

with

$$\begin{aligned} C_{\alpha\beta\gamma}^{S^\pm} = & \frac{-e^2}{2\sqrt{2}s_w^2} \left[v_d R_S^{1\alpha} R_{S^\pm}^{1\beta} R_{S^\pm}^{1\gamma} + (v_d R_S^{2\alpha} + v_u R_S^{1\alpha}) R_{S^\pm}^{1\beta} R_{S^\pm}^{2\gamma} \right. \\ & + v_u R_S^{2\alpha} R_{S^\pm}^{2\beta} R_{S^\pm}^{2\gamma} + (v_d R_S^{(2+i)\alpha} + v_{\nu_i} R_S^{1\alpha}) R_{S^\pm}^{(2+i)\beta} R_{S^\pm}^{1\gamma} \\ & \left. + (v_u R_S^{(2+i)\alpha} + v_{\nu_i} R_S^{2\alpha}) R_{S^\pm}^{(2+i)\beta} R_{S^\pm}^{2\gamma} + v_{\nu_i} R_S^{(2+j)\alpha} R_{S^\pm}^{(2+i)\beta} R_{S^\pm}^{(2+j)\gamma} \right] \\ & + \frac{e^2}{4\sqrt{2}s_w^2 c_w^2} (v_d R_S^{1\alpha} - v_u R_S^{2\alpha} + v_{\nu_i} R_S^{(2+i)\alpha}) [(c_w^2 - s_w^2) \delta^{\beta\gamma} \\ & - 2(c_w^2 - s_w^2) R_{S^\pm}^{2\beta} R_{S^\pm}^{2\gamma} - (c_w^2 - 3s_w^2) R_{S^\pm}^{(5+j)\beta} R_{S^\pm}^{(5+j)\gamma}] \\ & - \frac{1}{\sqrt{2}} \lambda_i \lambda_j v_{\nu_i} R_S^{(5+j)\alpha} [R_{S^\pm}^{1\beta} R_{S^\pm}^{1\gamma} + R_{S^\pm}^{2\beta} R_{S^\pm}^{2\gamma}] \\ & + \frac{1}{\sqrt{2}} \lambda_i Y_{\nu_{kj}} (v_{\nu_i} R_S^{(5+j)\alpha} + v_{\nu_j} R_S^{(5+i)\alpha}) R_{S^\pm}^{(2+k)\beta} R_{S^\pm}^{1\gamma} \\ & + \frac{1}{\sqrt{2}} \lambda_k Y_{e_{ij}} (v_{\nu_i} R_S^{(5+k)\alpha} + v_{\nu_k} R_S^{(2+i)\alpha}) R_{S^\pm}^{2\beta} R_{S^\pm}^{(5+j)\gamma} \\ & + \frac{1}{\sqrt{2}} \lambda_k Y_{e_{ij}} (v_u R_S^{(5+k)\alpha} + v_{\nu_k} R_S^{2\alpha}) R_{S^\pm}^{(2+i)\beta} R_{S^\pm}^{(5+j)\gamma} \\ & - \frac{1}{\sqrt{2}} Y_{\nu_{ki}} v_{\nu_i} R_S^{(5+j)\alpha} [Y_{\nu_{lj}} R_{S^\pm}^{(2+l)\beta} R_{S^\pm}^{(2+k)\gamma} + Y_{\nu_{kj}} R_{S^\pm}^{2\beta} R_{S^\pm}^{2\gamma}] \\ & + \frac{1}{\sqrt{2}} Y_{e_{ki}} Y_{e_{kj}} [v_d R_S^{1\alpha} (R_{S^\pm}^{(2+i)\beta} R_{S^\pm}^{(2+j)\gamma} - R_{S^\pm}^{(5+i)\beta} R_{S^\pm}^{(5+j)\gamma}) \\ & - (v_d R_S^{(2+i)\alpha} + v_{\nu_i} R_S^{1\alpha}) R_{S^\pm}^{(2+j)\beta} R_{S^\pm}^{1\gamma} + v_{\nu_i} R_S^{(2+j)\alpha} R_{S^\pm}^{1\beta} R_{S^\pm}^{1\gamma}] \\ & + \frac{1}{\sqrt{2}} Y_{e_{ki}} Y_{\nu_{kj}} (v_d R_S^{(5+i)\alpha} + v_{\nu_i} R_S^{1\alpha}) R_{S^\pm}^{2\beta} R_{S^\pm}^{(5+j)\gamma} \\ & + \frac{1}{\sqrt{2}} Y_{e_{ki}} Y_{\nu_{kj}} (v_u R_S^{(5+i)\alpha} + v_{\nu_i} R_S^{2\alpha}) R_{S^\pm}^{1\beta} R_{S^\pm}^{(5+j)\gamma} \\ & - \frac{1}{\sqrt{2}} [Y_{\nu_{ji}} (v_u R_S^{(2+j)\alpha} + v_{\nu_j} R_S^{2\alpha}) - \lambda_i (v_d R_S^{2\alpha} + v_u R_S^{1\alpha}) \\ & + 2\kappa_{ijk} v_{\nu_j} R_S^{(2+k)\alpha}] (Y_{\nu_i} R_{S^\pm}^{(2+l)\beta} R_{S^\pm}^{2\gamma} - \lambda_i R_{S^\pm}^{1\beta} R_{S^\pm}^{2\gamma}) \\ & + \frac{1}{\sqrt{2}} (A_\nu Y_\nu)_{ij} R_S^{(5+i)\alpha} R_{S^\pm}^{2\beta} R_{S^\pm}^{(2+j)\gamma} + \frac{1}{\sqrt{2}} (A_\lambda \lambda)_i R_S^{(5+i)\alpha} R_{S^\pm}^{2\beta} R_{S^\pm}^{1\gamma} \\ & + \frac{1}{\sqrt{2}} (A_e Y_e)_{ij} [R_S^{(2+i)\alpha} R_{S^\pm}^{(5+j)\beta} R_{S^\pm}^{1\gamma} - R_S^{1\alpha} R_{S^\pm}^{(5+j)\beta} R_{S^\pm}^{(2+i)\gamma}]. \quad (\text{B2}) \end{aligned}$$

The unitary matrices R_S , R_{S^\pm} (and R_u , R_d , Z_+ , Z_- below) can be found in Ref. [13].

The couplings between CP-even neutral scalars and squarks are written as

$$\mathcal{L}_{int} = \sum_{\alpha=1}^8 \sum_{I,J=1}^6 (C_{\alpha IJ}^{U^\pm} S_\alpha U_I^- U_J^+ + C_{\alpha IJ}^{D^\pm} S_\alpha D_I^+ D_J^-), \quad (\text{B3})$$

with

$$\begin{aligned} C_{\alpha IJ}^{U^\pm} = & \frac{-e^2}{6\sqrt{2}} (v_d R_S^{1\alpha} - v_u R_S^{2\alpha} - v_{\nu_j} R_S^{(2+j)\alpha}) \left[\frac{4}{c_W^2} \delta^{IJ} - \frac{3 + 2s_W^2}{s_W^2 c_W^2} R_u^{iI*} R_u^{iJ} \right] \\ & - \frac{1}{\sqrt{2}} \left[(A_u Y_u)_{ij} R_S^{2\alpha} - Y_{u_{ij}} \lambda_k (v_d R_S^{(5+k)\alpha} + v_{\nu_k} R_S^{1\alpha}) \right. \\ & \left. + Y_{u_{ij}} Y_{\nu_{kl}} (v_{\nu_k} R_S^{(5+l)\alpha} + v_{\nu_l} R_S^{(2+k)\alpha}) \right] (R_u^{iI*} R_u^{(3+j)J} + R_u^{(3+i)I*} R_u^{jJ}) \\ & - \sqrt{2} v_u Y_{u_{ik}} Y_{u_{jk}} R_S^{2\alpha} (R_u^{iI*} R_u^{jJ} + R_u^{(3+i)I*} R_u^{(3+j)J}), \end{aligned} \quad (\text{B4})$$

$$\begin{aligned} C_{\alpha IJ}^{D^\pm} = & \frac{e^2}{6\sqrt{2}} (v_d R_S^{1\alpha} - v_u R_S^{2\alpha} - v_{\nu_j} R_S^{(2+j)\alpha}) \left[\frac{2}{c_W^2} \delta^{IJ} - \frac{1 + 2s_W^2}{s_W^2 c_W^2} R_u^{iI*} R_u^{iJ} \right] \\ & - \frac{1}{\sqrt{2}} (A_d Y_d)_{ij} R_S^{1\alpha} (R_d^{iI*} R_d^{(3+j)J} + R_d^{(3+i)I*} R_d^{jJ}) \\ & + \frac{1}{\sqrt{2}} Y_{d_{ij}} \lambda_k (v_u R_S^{(5+k)\alpha} + v_{\nu_k} R_S^{2\alpha}) (R_d^{iI*} R_d^{(3+j)J} + R_d^{(3+i)I*} R_d^{jJ}) \\ & - \sqrt{2} v_d Y_{d_{ik}} Y_{d_{jk}} R_S^{1\alpha} (R_d^{iI*} R_d^{jJ} + R_d^{(3+i)I*} R_d^{(3+j)J}). \end{aligned} \quad (\text{B5})$$

The interaction Lagrangian between CP-even neutral scalars and charginos is formulated as

$$\mathcal{L}_{int} = \sum_{\alpha=1}^8 \sum_{\beta,\gamma=1}^2 S_\alpha \bar{\chi}_\beta^+ \left(C_{\alpha\beta\gamma}^{\chi^\pm} P_L + [C_{\alpha\beta\gamma}^{\chi^\pm}]^* P_R \right) \chi_\gamma^-, \quad (\text{B6})$$

where

$$\begin{aligned} C_{\alpha\beta\gamma}^{\chi^\pm} = & \frac{-e}{\sqrt{2} s_W} \left[R_S^{1\alpha} Z_+^{1\beta} Z_-^{2\gamma} + R_S^{2\alpha} Z_+^{2\beta} Z_-^{1\gamma} + R_S^{(2+i)\alpha} Z_+^{1\beta} Z_-^{(2+i)\gamma} \right] \\ & - \frac{Y_{e_{ij}}}{\sqrt{2}} \left[R_S^{1\alpha} Z_+^{(2+i)\beta} Z_-^{(2+j)\gamma} - R_S^{(2+i)\alpha} Z_+^{(2+j)\beta} Z_-^{1\gamma} \right] \\ & - \frac{Y_{\nu_{ij}}}{\sqrt{2}} R_S^{(5+i)\alpha} Z_+^{2\beta} Z_-^{(2+j)\gamma} - \frac{\lambda_i}{\sqrt{2}} R_S^{(5+i)\alpha} Z_+^{2\beta} Z_-^{2\gamma}, \end{aligned} \quad (\text{B7})$$

and

$$P_L = \frac{1}{2}(1 - \gamma_5), \quad P_R = \frac{1}{2}(1 + \gamma_5). \quad (\text{B8})$$

Appendix C: Form factors

The form factors are

$$A_0(x) = -(x - g(x))/x^2, \quad (C1)$$

$$A_{1/2}(x) = 2[x + (x - 1)g(x)]/x^2, \quad (C2)$$

$$A_1(x) = -[2x^2 + 3x + 3(2x - 1)g(x)]/x^2, \quad (C3)$$

with

$$g(x) = \begin{cases} \arcsin^2 \sqrt{x}, & x \leq 1; \\ -\frac{1}{4} \left[\ln \frac{1 + \sqrt{1-1/x}}{1 - \sqrt{1-1/x}} - i\pi \right]^2, & x > 1, \end{cases} \quad (C4)$$

and

$$F(x) = -(1 - x^2) \left(\frac{47}{2} x^2 - \frac{13}{2} + \frac{1}{x^2} \right) - 3(1 - 6x^2 + 4x^4) \ln x \\ + \frac{3(1 - 8x^2 + 20x^4)}{\sqrt{4x^2 - 1}} \cos^{-1} \left(\frac{3x^2 - 1}{2x^3} \right). \quad (C5)$$

Appendix D: Minimisation of the potential

In the basis $S^T = (h_d, h_u, (\tilde{\nu}_i)^\Re, (\tilde{\nu}_i^c)^\Re)$, the tree-level neutral scalar potential contains the following linear terms [3]

$$V_{\text{linear}}^0 = t_{h_d}^0 h_d + t_{h_u}^0 h_u + t_{(\tilde{\nu}_i)^\Re}^0 (\tilde{\nu}_i)^\Re + t_{(\tilde{\nu}_i^c)^\Re}^0 (\tilde{\nu}_i^c)^\Re, \quad (D1)$$

where the different t^0 are the tadpoles at tree-level. They are equal to zero at the minimum of the tree-level potential, and are given by

$$t_{h_d}^0 = m_{H_d}^2 v_d + \frac{G^2}{4} (v_d^2 - v_u^2 + v_{\nu_i} v_{\nu_i}) v_d - (A_\lambda \lambda)_i v_u v_{\nu_i^c} - \lambda_j \kappa_{ijk} v_u v_{\nu_i^c} v_{\nu_k^c} \\ + (\lambda_i \lambda_j v_{\nu_i^c} v_{\nu_j^c} + \lambda_i \lambda_i v_u^2) v_d - Y_{\nu_{ij}} v_{\nu_i} (\lambda_k v_{\nu_k^c} v_{\nu_j^c} + \lambda_j v_u^2), \quad (D2)$$

$$t_{h_u}^0 = m_{H_u}^2 v_u - \frac{G^2}{4} (v_d^2 - v_u^2 + v_{\nu_i} v_{\nu_i}) v_u + (A_\nu Y_\nu)_{ij} v_{\nu_i} v_{\nu_j^c} - (A_\lambda \lambda)_i v_d v_{\nu_i^c} \\ + (\lambda_i \lambda_j v_{\nu_i^c} v_{\nu_j^c} + \lambda_i \lambda_i v_u^2) v_u + Y_{\nu_{ij}} v_{\nu_i} (\kappa_{ljk} v_{\nu_l^c} v_{\nu_k^c} - 2\lambda_j v_d v_u) \\ - \lambda_j \kappa_{ijk} v_d v_{\nu_i^c} v_{\nu_k^c} + (Y_{\nu_{ki}} Y_{\nu_{kj}} v_{\nu_i^c} v_{\nu_j^c} + Y_{\nu_{ik}} Y_{\nu_{jk}} v_{\nu_i} v_{\nu_j}) v_u, \quad (D3)$$

$$\begin{aligned}
t_{(\bar{\nu}_i)\Re}^0 &= m_{L_{ij}}^2 v_{\nu_j} + \frac{G^2}{4}(v_d^2 - v_u^2 + v_{\nu_j} v_{\nu_j}) v_{\nu_i} + (A_\nu Y_\nu)_{ij} v_u v_{\nu_j}^c \\
&\quad - Y_{\nu_{ij}} \lambda_k v_{\nu_j}^c v_{\nu_k}^c v_d - Y_{\nu_{ij}} \lambda_j v_u^2 v_d + Y_{\nu_{il}} \kappa_{ljk} v_u v_{\nu_j}^c v_{\nu_k}^c \\
&\quad + Y_{\nu_{ij}} Y_{\nu_{lk}} v_{\nu_l} v_{\nu_j}^c v_{\nu_k}^c + Y_{\nu_{ik}} Y_{\nu_{jk}} v_u^2 v_{\nu_j}, \tag{D4}
\end{aligned}$$

$$\begin{aligned}
t_{(\bar{\nu}_i^c)\Re}^0 &= m_{\bar{\nu}_{ij}^c}^2 v_{\nu_j}^c + (A_\nu Y_\nu)_{ji} v_{\nu_j} v_u - (A_\lambda \lambda)_i v_d v_u + (A_\kappa \kappa)_{ijk} v_{\nu_j}^c v_{\nu_k}^c \\
&\quad + \lambda_i \lambda_j v_{\nu_j}^c (v_d^2 + v_u^2) + 2\kappa_{lim} \kappa_{ljk} v_{\nu_m}^c v_{\nu_j}^c v_{\nu_k}^c - 2\lambda_j \kappa_{ijk} v_d v_u v_{\nu_k}^c \\
&\quad - Y_{\nu_{ji}} \lambda_k v_{\nu_j} v_{\nu_k}^c v_d - Y_{\nu_{kj}} \lambda_i v_{\nu_k} v_{\nu_j}^c v_d + 2Y_{\nu_{jk}} \kappa_{ikl} v_u v_{\nu_j} v_{\nu_l}^c \\
&\quad + Y_{\nu_{ji}} Y_{\nu_{lk}} v_{\nu_j} v_{\nu_l} v_{\nu_k}^c + Y_{\nu_{ki}} Y_{\nu_{kj}} v_u^2 v_{\nu_j}^c. \tag{D5}
\end{aligned}$$

-
- [1] H.P. Nilles, *Phys. Rep.* **110** (1984) 1; H.E. Haber and G.L. Kane, *Phys. Rept.* **117** (1985) 75; H.E. Haber, arXiv:hep-ph/9306207; S.P. Martin, arXiv:hep-ph/9709356; J. Rosiek, *Phys. Rev.* **D 41** (1990) 3464 [hep-ph/9511250].
- [2] D.E. López-Fogliani and C. Muñoz, *Phys. Rev. Lett.* **97** (2006) 041801 [hep-ph/0508297].
- [3] N. Escudero, D.E. López-Fogliani, C. Muñoz and R. Ruiz de Austri, *JHEP* **12** (2008) 099 [arXiv:0810.1507]; J. Fidalgo, D.E. López-Fogliani, C. Muñoz and R. Ruiz de Austri, *JHEP* **10** (2011) 020 [arXiv:1107.4614].
- [4] P. Bandyopadhyay, P. Ghosh and S. Roy, *Phys. Rev.* **D 84** (2011) 115022 [arXiv:1012.5762]; P. Ghosh, D.E. López-Fogliani, V.A. Mitsou, C. Muñoz and R. Ruiz de Austri, *Phys. Rev.* **D 88** (2013) 015009 [arXiv:1211.3177].
- [5] J.E. Kim and H.P. Nilles, *Phys. Lett.* **B 138** (1984) 150.
- [6] P. Ghosh and S. Roy, *JHEP* **04** (2009) 069 [arXiv:0812.0084]; A. Bartl, M. Hirsch, S. Liebler, W. Porod and A. Vicente, *JHEP* **05** (2009) 120 [arXiv:0903.3596]; J. Fidalgo, D.E. López-Fogliani, C. Muñoz and R. Ruiz de Austri, *JHEP* **08** (2009) 105 [arXiv:0904.3112]; P. Ghosh, P. Dey, B. Mukhopadhyaya and S. Roy, *JHEP* **05** (2010) 087 [arXiv:1002.2705].
- [7] F. Englert and R. Brout, *Phys. Rev. Lett.* **13** (1964) 321; P. W. Higgs, *Phys. Lett.* **12** (1964) 132; P. W. Higgs, *Phys. Rev. Lett.* **13** (1964) 508; G. Guralnik, C. Hagen, and T. Kibble, *Phys. Rev. Lett.* **13** (1964) 585.
- [8] ATLAS Collaboration, *Phys. Lett.* **B 716** (2012) 1 [arXiv:1207.7214].

- [9] CMS Collaboration, *Phys. Lett. B* **716** (2012) 30 [arXiv:1207.7235].
- [10] ATLAS Collaboration, ATLAS-CONF-2012-135; ATLAS Collaboration, *Phys. Lett. B* **718** (2012) 369 [arXiv:1207.0210]; ATLAS Collaboration, *JHEP* **09** (2012) 070 [arXiv:1206.5971]; ATLAS Collaboration, ATLAS-CONF-2013-014; ATLAS Collaboration, ATLAS-CONF-2013-034; ATLAS Collaboration, ATLAS-CONF-2013-040.
- [11] CMS Collaboration, CMS-PAS-HIG-12-025; CMS Collaboration, CMS-PAS-HIG-13-004; CMS Collaboration, CMS-PAS-HIG-13-005.
- [12] H.-B. Zhang, T.-F. Feng, S.-M. Zhao and T.-J. Gao, *Nucl. Phys. B* **873** (2013) 300 [arXiv:1304.6248].
- [13] H.-B. Zhang, T.-F. Feng, G.-F. Luo, Z.-F. Ge and S.-M. Zhao, *JHEP* **07** (2013) 069 [Erratum *ibid.* **10** (2013) 173] [arXiv:1305.4352].
- [14] M. Carena, J.R. Espinosa, M. Quirós and C.E.M. Wagner, *Phys. Lett. B* **355** (1995) 209 [hep-ph/9504316]; M. Carena, M. Quirós and C.E.M. Wagner, *Nucl. Phys. B* **461** (1996) 407 [hep-ph/9508343]; M. Carena, S. Gori, N.R. Shahb and C.E.M. Wagner, *JHEP* **03** (2012) 014 [arXiv:1112.3336].
- [15] H.E. Haber and R. Hempfling, *Phys. Rev. D* **48** (1993) 4280.
- [16] P.P. Giardino, K. Kannike, I. Masina, M. Raidal and A. Strumia, CERN-PH-TH-2013-052, arXiv:1303.3570.
- [17] C. Anastasiou and K. Melnikov, *Nucl. Phys. B* **646** (2002) 220.
- [18] J.R. Ellis, M.K. Gaillard and D.V. Nanopoulos, *Nucl. Phys. B* **106** (1976) 292; M.A. Shifman, A.I. Vainshtein, M.B. Voloshin and V.I. Zakharov, *Sov. J. Nucl. Phys.* **30** (1979) 711; A. Djouadi, *Phys. Rept.* **459** (2008) 1 [hep-ph/0503173]; J.F. Gunion, H.E. Haber, G.L. Kane and S. Dawson, *Front. Phys.* **80** (2000) 1; M. Carena, I. Low and C.E.M. Wagner, *JHEP* **08** (2012) 060 [arXiv:1206.1082]; T.-F. Feng, S.-M. Zhao, H.-B. Zhang, Y.-J. Zhang and Y.-L. Yan, *Nucl. Phys. B* **871** (2013) 223 [arXiv:1303.0047].
- [19] W.-Y. Keung and W.J. Marciano, *Phys. Rev. D* **30** (1984) 248.
- [20] L. Resnick, M.K. Sundaresan, P.J.S. Watson, *Phys. Rev. D* **8** (1973) 172; J.F. Gunion, H.E. Haber, *Nucl. Phys. B* **272** (1986) 1 [hep-ph/9301205].
- [21] A. Arbey, A. Deandrea, F. Mahmoudi, A. Tarhini, *Phys. Rev. D* **87** (2013) 115020

- [arXiv:1304.0381].
- [22] T. Aaltonen et al., CDF and D0 Collaborations, *Phys. Rev. Lett.* **109** (2012) 071804 [arXiv:1207.6436].
- [23] CMS Collaboration, CMS-PAS-HIG-2012-004; CMS Collaboration, CMS-PAS-HIG-2012-044.
- [24] ATLAS Collaboration, ATLAS-CONF-2012-161.
- [25] ATLAS Collaboration, ATLAS-CONF-2013-012.
- [26] CMS Collaboration, CMS-PAS-HIG-13-001.
- [27] ATLAS Collaboration, ATLAS-CONF-2013-013.
- [28] CMS Collaboration, CMS-PAS-HIG-13-002.
- [29] ATLAS Collaboration, ATLAS-CONF-2013-030.
- [30] CMS Collaboration, CMS-PAS-HIG-13-003.
- [31] J. Beringer et al., Particle Data Group, *Phys. Rev. D* **86** (2012) 010001.
- [32] B. Pontecorvo, *Sov. Phys. JETP* **7** (1958) 172, *Zh. Eksp. Teor. Fiz.* **34** (1957) 247; Z. Maki, M. Nakagawa and S. Sakata, *Prog. Theor. Phys.* **28** (1962) 870.
- [33] K. Abe et al., T2K Collaboration, *Phys. Rev. Lett.* **107** (2011) 041801 [arXiv:1106.2822]; P. Adamson et al., MINOS Collaboration, *Phys. Rev. Lett.* **107** (2011) 181802 [arXiv:1108.0015]; Y. Abe et al., DOUBLE-CHOOZ Collaboration, *Phys. Rev. Lett.* **108** (2012) 131801 [arXiv:1112.6353]; F. An et al., DAYA-BAY Collaboration, *Phys. Rev. Lett.* **108** (2012) 171803 [arXiv:1203.1669]; J. Ahn et al., RENO Collaboration, *Phys. Rev. Lett.* **108** (2012) 191802 [arXiv:1204.0626].
- [34] M. Gonzalez-Garcia, M. Maltoni, J. Salvado, and T. Schwetz, *JHEP* **12** (2012) 123 [arXiv:1209.3023]; D.V. Forero, M. Tórtola and J.W.F. Valle, *Phys. Rev. D* **86** (2012) 073012 [arXiv:1205.4018].
- [35] S.M. Bilenky, J. Hosek, and S.T. Petcov, *Phys. Lett. B* **94** (1980) 495; J. Schechter and J.W.F. Valle, *Phys. Rev. D* **22** (1980) 2227; M. Doi, T. Kotani, H. Nishiura, K. Okuda, and E. Takasugi, *Phys. Lett. B* **102** (1981) 323.
- [36] J. Barea, J. Kotila and F. Iachello, *Phys. Rev. Lett.* **109** (2012) 042501.
- [37] P.A.R. Ade et al., Planck Collaboration, arXiv:1303.5076.
- [38] E821: G.W. Bennett et al., [Muon (g-2) Collaboration], *Phys. Rev. D* **73** (2006) 072003; Peter

- J. Mohr, Barry N. Taylor, David B. Newell, *Rev. Mod. Phys.* **80** (2008) 633.
- [39] ATLAS Collaboration, *Phys. Lett. B* **715** (2012) 44; ATLAS Collaboration, ATLAS-CONF-2013-025; CMS Collaboration, CMS-PAS-SUS-13-014.
- [40] M. Carena, G. Nardini, M. Quirós and C.E.M. Wagner, *JHEP* **10** (2008) 062 [arXiv:0806.4297].
- [41] CMS Collaboration, *Phys. Lett. B* **710** (2012) 26; ATLAS Collaboration, ATLAS-CONF-2013-067.
- [42] A. Arvanitaki and G. Villadoro, *JHEP* **02** (2012) 144 [arXiv:1112.4835].
- [43] K. Blum, R.T. D’Agnolo and J. Fan, *JHEP* **01** (2013) 057 [arXiv:1206.5303].
- [44] M.R. Buckley and D. Hooper, *Phys. Rev. D* **86** (2012) 075008 [arXiv:1207.1445].
- [45] J.R. Espinosa, C. Grojean, V. Sanz and M. Trott, *JHEP* **12** (2012) 077 [arXiv:1207.7355].
- [46] M. Carena, S. Gori, N.R. Shahb, C.E.M. Wagner and L.-T. Wang, *JHEP* **08** (2013) 087 [arXiv:1303.4414].
- [47] M. Carena, S. Gori, N.R. Shahb, C.E.M. Wagner and L.-T. Wang, *JHEP* **07** (2012) 175 [arXiv:1205.5842].
- [48] J.R. Ellis, G. Ridolfi and F. Zwirner, *Phys. Lett. B* **257** (1991) 83; J.R. Ellis, G. Ridolfi and F. Zwirner, *Phys. Lett. B* **262** (1991) 477; R. Barbieri and M. Frigeni, *Phys. Lett. B* **258** (1991) 395; M. Drees and M.M. Nojiri, *Phys. Rev. D* **45** (1992) 2482; M.A. Diaz and H.E. Haber, *Phys. Rev. D* **46** (1992) 3086; J.A. Casas, J.R. Espinosa, M. Quiros and A. Riotto, *Nucl. Phys. B* **436** (1995) 3 [*Erratum-ibid.* **B 439** (1995) 466].